Optimized Power Allocation for a Cooperative NOMA System with SWIPT and an Energy-Harvesting User

Carla E. Garcia , Pham Viet Tuan , Mario R. Camana & Insoo Koo

Taylor & Francis
Taylor & Francis Group

Check for updates

Optimized Power Allocation for a Cooperative NOMA System with SWIPT and an Energy-Harvesting User

Carla E. Garcia [ID][a], Pham Viet Tuan[b], Mario R. Camana[a] and Insoo Koo[a]

[a]School of Electrical and Computer Engineering, University of Ulsan, Ulsan, South Korea; [b]Faculty of Physics, University of Education, Hue University, Vietnam

ABSTRACT

This paper investigates the solution to an optimisation problem to minimise the total transmission power at the transmitter in a cooperative non-orthogonal multiple access (NOMA) system with simultaneous wireless information and power transfer (SWIPT) and an energy-harvesting user. First, we formulate the optimisation problem to obtain the minimum transmission power at the transmitter under the constraints of minimum signal-to-interference-plus-noise ratio and minimum energy harvesting. Since the problem is not convex, we transform it into a bi-level optimisation problem. Then, conditions to guarantee the feasibility of the problem are provided, and we derive the analytical optimal solution via the Lagrange method meeting Karush–Kuhn–Tucker optimality conditions to solve the lower-level variables of the inner convex problem. Second, we use particle swarm optimisation to find the approximately optimal values of the upper-level variables. Next, we present two baseline schemes based on orthogonal multiple access (OMA) and equal power splitting for performance comparison with the proposed cooperative NOMA system with SWIPT. Finally, simulation results show that cooperative NOMA with SWIPT can reduce the transmit power at the transmitter, compared to two baseline schemes: OMA and EPS.

1. Introduction

Non-orthogonal multiple access (NOMA) has aroused great interest in the fifth-generation (5G) networks because it achieves higher spectral efficiency in comparison with conventional orthogonal multiple access (OMA) (Ding, Lei et al., 2017, October), particularly to aid massive connectivity and to meet requirements of the Internet of Things (IoT) (Ding, Liu et al., 2017, February). NOMA can be divided into two types, namely code-domain and power domain. In this paper, we focus on power-domain multiplexing technique, which allows performing multiple access between multiple users when they share the same resource elements (e.g. spreading codes, time slots and frequency bands), in this way, this transmission strategy permits efficient use of the spectrum (Chen et al., 2017, October; Liu et al., 2017, December).

The enabling techniques for NOMA are superposition coding at the transmitter and successive interference cancellation (SIC) at the receiver (Islam et al., 2017). Basically, the transmitter broadcasts a superposition signal, which corresponds to the sum of all the messages of the users with different power allocation coefficients; thereby, NOMA ensures that the weaker users get a superior portion of the total power budget (Hanif et al., 2016, January). By applying SIC, a user with strong channel conditions can remove interference from a user with a weaker channel, since the strong-channel user first decodes the message of the weaker one, and then decodes its own message (Lv et al., 2018, April). The one with poor channel conditions decodes a message by treating the other message as noise. In this way, users with strong and poor channel conditions can access all resource blocks (Chen et al., 2017, October).

Ding et al. (2015, August) proposed and analysed a new cooperative NOMA scheme in order to improve the reliability of distant users since users both near to and distant from the base station (BS) co-exist, this entails performance degradation for distant users. Therefore, the main idea of this cooperative transmission strategy in NOMA systems is that the users with the best channel conditions (i.e. those that are close to the BS) are employed as relays to help users with poor channel conditions. However, there is compensation between information forwarding and information receiving because of the limited energy storage at the relay nodes, especially in order to meet IoT functionality requirements (Zhai et al., 2018, June). Therefore, several efforts have been made to implement energy harvesting (EH)-wireless networks, which provides self-sustainability and the possibility of sharing energy among the nodes. To this end, wireless power transfer (WPT) is one of the EH technologies capable of providing controllable and continuous power supply, different from solar or wind energy harvesting resources, which are unreliable and intermittent. In WPT, energy can be harvested from electromagnetic radiation. Subsequently, the terminals with WPT function may harvest energy opportunistically from a dedicated fully controlled power source that intentionally transmits electromagnetic energy or from ambient electromagnetic sources (Krikidis et al., 2014, November). Wireless-powered communication networks (WPCNs) can remotely replenish the battery of the wireless communication devices by utilising microwave WPT technology. In this sense, WPCN does not need replacement or recharging of the battery, which can improve communication performance and reduce the operational cost. Therefore, WPCN is mainly suitable for low-power applications such as radio frequency identification (RFID) networks and wireless sensor networks (WSNs) in which devices can operate with power up to several (Bi, Zeng & Zhang, 2016, April).

WPCN with NOMA was investigated by Diamantoulakis et al. (2016, December). In the study, it was shown that NOMA provides a considerable improvement in user fairness, and throughput in comparison with orthogonal conventional schemes. Diamantoulakis et al. (2017, January) also had compared the performance of NOMA and time-division multiple access (TDMA) to optimise the downlink and uplink users' rates of a wireless powered network by considering the cascade near-far problem with interference. The results showed that NOMA outperforms TDMA in the downlink especially when the users locate at different distances from the BS and when interference power level is low. Despite the benefits provided by WPT to wireless communication networks such as uninterrupted operation with sensors, radio waves carry both energy and information simultaneously. Wireless information and power transmission (WIPT) technology is a unified system for

transferring power and information simultaneously, which improves the network infrastructure to energise and enhance the use of radio frequency (RF) spectrum and radiation (Clerckx et al., 2019, January). WIPT can be classified into three different types: simultaneous wireless information and power transfer (SWIPT), wirelessly powered communication network (WPCN) and wirelessly powered backscatter communication (WPBC).

Recently, SWIPT has aroused interest in researching different types of energy-efficient network (Ponnimbaduge Perera et al., 2018; Shi et al., 2016, February). SWIPT has been envisaged for aiding power-limited battery-driven devices (Zhou et al., 2018, April), and it provides another choice in energy-harvesting (EH) techniques because it allows simultaneous information decoding (ID) for the user and radio frequency (RF) energy harvesting (Camana et al., 2018, November). Cooperative NOMA with SWIPT is also considered as a promising technology for future wireless communication networks (Do et al., 2017, March). It was investigated by Liu et al. (2016, April) to alleviate energy constraints in which users that are close to the BS perform SWIPT while acting as EH relays to enhance the reliability of distant users (i.e. those with worse channel conditions) without consuming the nearer users' batteries in a single-input single-output (SISO) scenario. Xu et al. (2017, September) investigated cooperative NOMA with SWIPT in multiple-input single-output (MISO) and SISO cases to maximise the data rate of the strong user, as well as guarantee the quality of service (QoS) requirements of the weak user. The application of SWIPT to cooperative cognitive radio NOMA (CR-NOMA) and NOMA with fixed power allocation (F-NOMA) was investigated by Yang et al. (2017, July), which is based on outage probabilities and diversity gain approximations, where all nodes have a single antenna, concluding that it is possible to reduce the outage probability through the application of the NOMA scheme. Alsaba et al. (2018) proposed a downlink cooperative NOMA with SWIPT, beamforming, and full-duplex techniques, which accomplished a higher sum rate than OMA beamforming systems and conventional non-cooperative NOMA.

Although SWIPT and cooperative NOMA systems have been investigated in the literature, as mentioned above, none of the researchers studied the transmission power minimisation problem considering an energy-harvester user.

Motivated by the fact that 5G communications and its relationship to the IoT has been growing increasingly, the potential application scenarios (e.g. massive machine-type communications) as well as the energy efficiency, low power and low cost entailed in the application of a SISO antenna configuration, these facts encouraged us to investigate SISO in cooperative NOMA with SWIPT.

In this paper, we focus on studying power allocation to minimise the total transmission power in a downlink cooperative NOMA system with SWIPT. In addition to NOMA users, we consider an energy-harvesting user that can be used for a low-power sensor or a low-power device for IoT applications.

The main contributions of this paper are summarised as follows:

- We provide the solution to the power allocation problem, which minimises the total transmission power for a downlink cooperative NOMA system with SWIPT and an additional EH user. From this, it is possible to guarantee the QoS requirements of the distant user and the nearby user under the constraint of minimum EH at user 3.
- The formulated problem to minimise the transmission power of the transmitter under the proposed scheme is non-convex and challenging to solve.

Consequently, we turned the initial problem into a bi-level optimisation problem and applied the Lagrange method to solve the inner optimisation problem, where variables are related to the control power variables, whilst an algorithm based on particle swarm optimisation (PSO) is used to solve the outer optimisation problem. We provide the conditions to guarantee the feasibility of the problem, and the analytical optimal solution performed by the Lagrange method is proven to satisfy all the Karush–Kuhn–Tucker (KKT) conditions.

- For performance comparison, we consider optimising power allocation for OMA strategy transmission. Similar to the case of cooperative NOMA with SWIPT, we also provided the solution to the power allocation scheme for OMA based on PSO and the Lagrange methods.

The rest of the paper is organised as follows. In Section 2, we describe the system model. In Section 3, we formulate the problem and present the solution to total transmission power minimisation for a cooperative NOMA system with SWIPT. For comparison purpose, the problem formulation and solution for OMA is developed in Section 4. Finally, numerical results and the conclusion are presented in Sections 5 and 6, respectively.

2. System model

We consider a cooperative NOMA transmission system with SWIPT, as shown in Figure 1, where the transmitter has one antenna, and there are three single-antenna users that are denoted user 1, user 2 and EH–user 3. Without loss of generality, we assume that nearby user 2 has better channel conditions than distant user 1 (e.g. user 2 is a cell-centre user, and user 1 is a cell-edge user). Thereby, user 2 can function as an EH relay to help and guarantee the QoS requirements of user 1.

Cooperative NOMA involves two phases: Phase A and Phase B. In Phase A, distant user 1 receives the signal from the transmitter, and nearby user 2 performs SWIPT, which consists of splitting the received signal into two parts (one for ID and the other for EH) based on a power-splitting ratio, β. In addition, user 3 is a RF energy harvesting device where the extraction of RF power is performed by receiving the superimposed RF signals of user 1 and user 2 through an antenna. Different from solar or wind energy which can be intermittent, the main advantage of RF energy harvesting is that it can be used for indoor and outdoor environments and can operate continuously during day and night (Nechibvute et al., 2017). In Phase B, user 2 retransmits message 1 to user 1 by using the harvested energy obtained in Phase A. Furthermore, user 1 utilises maximal-ratio combination (MRC) to merge the message received in the two phases and then decodes it. In the following subsection, we provide operations of Phase A and B in more details.

2.1. Phase A: direct transmission

In this phase, the transmitter sends the signal, $s = w_1 s_1 + w_2 s_2 + w_3 s_3$, where $s_1, s_2 \in \mathbb{C}$ are the independent and identically distributed (*i.i.d.*) information bearing messages for user 1 and user 2, respectively; s_3 carries a known symbol. Since the energy signal of s_3 carries no information, s_3 can be assigned as an arbitrary random signal or be known signal to both the transmitter and the user prior to information transmission (Xu et al., 2014). The power of the
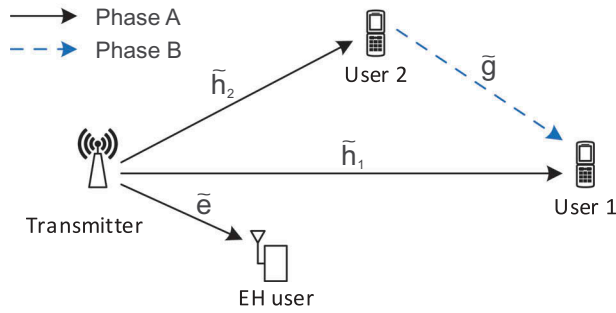
Figure 1. Transmission under cooperative NOMA with SWIPT.

transmitted symbol is normalised, i.e. $E(|s_1|^2) = E(|s_2|^2) = E(|s_3|^2) = 1$, and w_1, w_2 and w_3 are the corresponding transmit power control variables.

The received signal at user 1 can be given as

$$y_1^{(A)} = \widetilde{h}_1(w_1s_1 + w_2s_2 + w_3s_3) + z_1^{(A)}, \tag{1}$$

where $\widetilde{h}_1$ is the channel coefficient between the transmitter and user 1, and $z_1^{(A)} \sim \mathcal{CN}(0, \sigma_1^2)$ is the average white Gaussian noise (AWGN) at user 1. Note that user 1 can cancel the interference from the known symbol s_3. Because of the interference caused by user 2, the received signal-to-interference-plus-noise ratio (SINR) at user 1 to detect s_1 can be described by (2):

$$SINR_{1,s_1}^{(A)} = \frac{h_1w_1^2}{h_1w_2^2 + 1}, \tag{2}$$

where $h_1 = \frac{|\widetilde{h}_1|^2}{\sigma_1^2}$.

The power splitting architecture employed to perform SWIPT for user 2 is represented in Figure 2. The received signal at user 2 is split into two streams, one stream with PS ratio $\beta \in (0, 1)$ is used for EH, and the other $(1 - \beta)$ is used for ID. With the power splitting architecture, the received signal for ID at user 2 can be described as shown in (3):
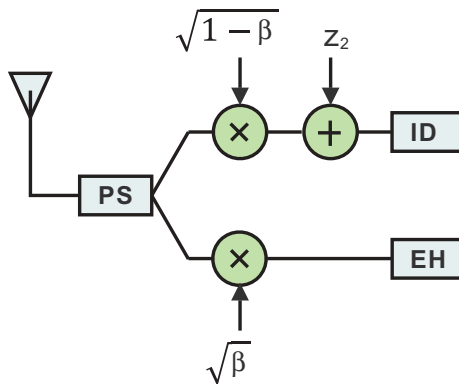

Figure 2. The power splitting architecture at the relay user 2.

$$y_2^{(A)} = \sqrt{1 - \beta}\,\widetilde{h}_2(w_1 s_1 + w_2 s_2 + w_3 s_3) + z_2^{(A)}, \tag{3}$$

where $\widetilde{h}_2$ is the channel coefficient between the transmitter and user 2, $z_2^{(A)} \sim \mathcal{CN}(0, \sigma_2^2)$ is the AWGN, $\beta \in (0, 1)$ is the power-splitting ratio and s_3 can be cancelled upon ID since s_3 is a known symbol.

In accordance with NOMA principles, SIC is carried out at nearby user 2. In particular, user 2 first decodes the message of distant user 1 and then subtracts this message from the received signal. Therefore, the SINR of user 2 to decode message 1 is expressed as

$$SINR_{2,s_1}^{(A)} = \frac{(1 - \beta)h_2 w_1^2}{(1 - \beta)h_2 w_2^2 + 1}, \tag{4}$$

where $h_2 = \frac{\left|\widetilde{h}_2\right|^2}{\sigma_2^2}$.

In the proposed work, we consider that user 2 can correctly perform SIC where the main condition is that the SINR at user 2 to decode message 1, denoted by $SINR_{2,s_1}^{(A)}$, should be larger than the target SINR of user 1 denoted by γ such that we have

$$\frac{(1 - \beta)h_2 w_1^2}{(1 - \beta)h_2 w_2^2 + 1} \geq \gamma. \tag{5}$$

Moreover, SIC receiver utilises the traditional decoder to decode the composite received signal at different phases. Therefore, in terms of hardware, the complexity of SIC receiver is architecturally similar to that of conventional non-SIC receiver (Mollanoori & Ghaderi, 2011; Tabassum, Ali, Hossain, Hossain et al., 2017).

Since user 2 subtracts the message of user 1, s_1, from $y_2^{(A)}$ to decode its own message, s_2, the SNR of user 2 is given by

$$SNR_{2,s_2}^{(A)} = (1 - \beta)h_2 w_2^2. \tag{6}$$

Finally, the energy harvested by nearby user 2 can be modelled as (Y. Xu et al., 2017, September)

$$E_2^{(A)} = \beta\left|\widetilde{h}_2\right|^2(w_1^2 + w_2^2 + w_3^2)\tau, \tag{7}$$

where $\tau \in (0, 1)$ is the transmission time fraction for Phase A. For simplicity, we assume that the harvested energy is only used for information forwarding while the energy consumption for signal processing and the circuit maintaining, etc., can be ignored (Liu et al., 2016, April). Subsequently, the transmit power at user 2, $P_{t,2}$ is expressed as

$$P_{t,2} = \frac{E_2^{(A)}}{1 - \tau} = \frac{\beta\left|\widetilde{h}_2\right|^2(w_1^2 + w_2^2 + w_3^2)\tau}{1 - \tau}. \tag{8}$$

With respect to user 3, the harvested energy can be expressed as

$$EH_3 = \left|\widetilde{e}\right|^2(w_1^2 + w_2^2 + w_3^2)\tau = e(w_1^2 + w_2^2 + w_3^2), \tag{9}$$

where $e = \left|\widetilde{e}\right|^2\tau$ and $\widetilde{e}$ is the channel coefficient from the transmitter to user 3.

2.2. *Phase B: cooperative transmission*

In this phase, user 2 retransmits message s_1 to user 1 utilising harvested energy. Therefore, the received signal at user 1 is expressed by

$$y_1^{(B)} = \sqrt{P_{t,2}}\tilde{g}s_1 + z_1^{(B)}, \tag{10}$$

where $\tilde{g}$ is the channel coefficient from user 2 to user 1, and $z_1^{(B)} \sim \mathcal{CN}(0, \sigma_1^2)$ is the AWGN at user 1. The SNR to detect s_1 is obtained by the ratio of the transmission power received from user 2 to the power of noise σ_1^2, which is shown as follows:

$$SNR_{1,s_1}^{(B)} = \frac{P_{t,2}|\tilde{g}|^2}{\sigma_1^2} = \beta g h_2 \left(w_1^2 + w_2^2 + w_3^2\right) \tag{11}$$

where $g = \frac{|\tilde{g}|^2 \sigma_2^2 \tau}{\sigma_1^2(1-\tau)}$.

At the end of Phase 2, user 1 decodes message s_1 jointly based on the signals received from the transmitter and user 2 by utilising MRC. Hence, the equivalent SINR at user 1 can be described as

$$SINR_{1,s_1}^{Total} = SINR_{1,s_1}^{(A)} + SNR_{1,s_1}^{(B)}$$

$$= \frac{h_1 w_1^2}{h_1 w_2^2} + 1 + \beta g h_2 \left(w_1^2 + w_2^2 + w_3^2\right). \tag{12}$$

3. Problem formulation and the solution of cooperative NOMA with SWIPT

In the paper, we focus on finding optimal power allocation at the transmitter to minimise transmit power in cooperative NOMA with SWIPT. This power allocation problem is equivalent to minimisation of $w_1^2 + w_2^2 + w_3^2$ under the constraint of minimum energy-harvesting at user 3 and quality of service for the minimum required SINR at user 1 and the minimum required SNR at user 2. Here, let us define $x = w_1^2$, $y = w_2^2$, and $z = w_3^2$. Subsequently, the problem can be formulated as (13). To our knowledge, the power allocation problem under the proposed system has not been investigated in other literatures yet.

$$P1: \min_{\{x,y,z,\beta\}} \quad x + y + z \tag{13a}$$

$$\text{s.t.} \quad \frac{h_1 x}{h_1 y + 1} + \beta g h_2 (x + y + z) \geq \gamma, \tag{13b}$$

$$\frac{(1 - \beta)h_2 x}{(1 - \beta)h_2 y + 1} \geq \gamma, \tag{13c}$$

$$(1 - \beta)h_2 y \geq \alpha, \tag{13d}$$

$$e(x + y + z) \geq \xi, \tag{13e}$$

$$0 < \beta < 1. \tag{13f}$$

Constraints (13b) and (13c) are to guarantee that s_1 is successfully decoded by user 1 and user 2, respectively. Constraint (13d) corresponds to the received SNR at user 2, which should be higher than the target SNR of user 2, denoted by a to ensure that the user can detect its own message, s_2. Constraint (13e) represents the minimum EH ξ required by user 3. Note that since user 1 is the weaker user in the paper, user 2 sends the message s_1 to user 1 aided by SWIPT. Subsequently, the user 1 receives its signal from the transmitter and user 2. Then, it is necessary to meet the target SINR γ to guarantee the successfully decode its message in both user 1 and user 2. User 2 is the stronger user, therefore it performs SIC. So that, the user 2 first decodes the message s_1 of user 1 and then decodes its own message s_2 without interference. If the target SNR a at user 2 is satisfied, the message of user 2 can be successfully decoded.

Optimisation problem P1 above is non-convex since the power-splitting ratio, β, is coupled with transmit powers x, y, z in constraints (13b), (13c) and (13d). According to Proposition 1 (Xu et al., 2017, September), the constraint (13b) can be equivalently rewritten as (14) and (15) by introducing an auxiliary variable, $a \geq 0$. The constraint (13c) can be rewritten as convex form as like (16).

$$h_1 x \geq a h_1 y + a, \tag{14}$$

$$\beta g h_2 (x + y + z) \geq \gamma - a, \tag{15}$$

$$h_2 x - \gamma h_2 y \geq \frac{\gamma}{1 - \beta}. \tag{16}$$

Therefore, P1 can be rewritten as the following problem form:

$$P2: \min_{\{x,y,z,\beta,a\}} x + y + z \tag{17a}$$

$$\text{s.t. } h_1 x \geq a h_1 y + a, \tag{17b}$$

$$\beta g h_2 (x + y + z) \geq \gamma - a, \tag{17c}$$

$$h_2 x - \gamma h_2 y \geq \frac{\gamma}{1 - \beta}, \tag{17d}$$

$$(1 - \beta) h_2 y \geq a, \tag{17e}$$

$$e(x + y + z) \geq \xi, \tag{17f}$$

$$0 < \beta < 1. \tag{17g}$$

Apparently, problem P2 is non-convex since power-splitting ratio β is coupled with transmit power control variables x, y, and z in constraint (17c) and with variable y in constraint (17e). Moreover, auxiliary variable, a is coupled with variable y in constraint (17b); thus, it cannot be solved directly. To overcome this difficulty, in this paper we transform the problem P2 into a bilevel optimisation problem as follows:

$$P3: \quad \min_{\beta,a} \left(h(\beta, a) = \min_{x,y,z} x + y + z \right) \tag{18a}$$

$$\text{s.t. } ah_1 y + a - h_1 x \leq 0, \tag{18b}$$

$$\frac{\gamma - a}{\beta g} - h_2(x + y + z) \leq 0, \tag{18c}$$

$$\frac{\gamma}{(1 - \beta)} - h_2 x + \gamma h_2 y \leq 0, \tag{18d}$$

$$\frac{a}{(1 - \beta)} - h_2 y \leq 0, \tag{18e}$$

$$\xi - e(x + y + z) \leq 0, \tag{18f}$$

$$x \geq 0, y \geq 0, z \geq 0, \tag{18g}$$

$$0 < \beta < 1, \tag{18h}$$

where $h(\beta, a)$ corresponds to the inner optimisation problem with respect to variables $x, y,$ and z. Here it is noteworthy that the upper-level variables β and a correspond to outer optimisation problem P3, while lower-level variables x, y, z correspond to inner optimisation problem P3 when a and β are given. Hence, the power-splitting ratio β is not coupled with transmit powers $x, y,$ and z in constraint (18c), and the auxiliary variable a is not coupled with variable y in constraint (18b). The key idea is to iteratively optimise the outer and inner optimisation problems. That is, the upper-level variables β, and a obtained by a PSO-based method, are the input parameters to solve the inner optimisation problem $h(\beta, a)$. Then, based in the previous solution, the variables β and a are updated by the PSO algorithm, which are again used to resolve the inner optimisation problem. This process will be repeated until convergence.

Since inner problem P3 is convex, we will obtain the optimal solution for power control variables x, y, z by using the Lagrange method. On the other hand, we will use a PSO-based method (Robinson & Rahmat-Samii, 2004; Zhang et al., 2015) to find the approximately optimal solutions related to upper-level variables β and a of outer optimisation problem P3.

In addition, for the performance comparison with OMA scheme later, here let us define the data rates at each user; in this sense, R_{1,s_1} and R_{2,s_2} represent the rates at user 1 and user 2, respectively.

$$R_{1,s_1} = \frac{1}{2} \log_2 \left(1 + SINR_{1,s_1}^{Total} \right), \text{ and} \tag{19}$$

$$R_{2,s_2} = \frac{1}{2} \log_2 \left(1 + SNR_{2,s_2}^{(A)} \right). \tag{20}$$

3.1. Solution for the inner minimisation problem

In the subsection 3.1, we propose the Lagrange-based scheme for solving the lower-level variables of the inner optimisation problem P3 by using Proposition 1.

Proposition 1: For the inner problem P3, we define the optimal solution to transmit power x, y, z as $x^*, y^* z^*$, respectively. According to the below proof, x^*, y^* and z^* can be given as following:

$$x^* = \max(x_1, x_2), \tag{21a}$$

$$y^* = \frac{a}{(1-\beta)h_2}, \tag{21b}$$

$$z^* = \begin{cases} \frac{\gamma-a}{\beta g h_2} - x^* - y^*, & \text{if } \xi - e\left(\frac{\gamma-a}{\beta g h_2}\right) \le 0, \\ \frac{\xi}{e} - x^* - y, & \text{otherwise}, \end{cases} \tag{21c}$$

subject to the following feasibility conditions:

$$\max(x_1, x_2) \le x_{1a}, \ \text{if } \xi - e\left(\frac{\gamma-a}{\beta g h_2}\right) \le 0, \tag{22a}$$

$$\max(x_1, x_2) \le x_{1b}, \ \text{if } \xi - e\left(\frac{\gamma-a}{\beta g h_2}\right) > 0, \tag{22b}$$

where

$$x_1 = \frac{\gamma}{(1-\beta)h_2}(a+1), \tag{23a}$$

$$x_2 = \frac{a\alpha}{(1-\beta)} + \left(\frac{a}{h_1}\right), \tag{23b}$$

$$x_{1a} = \frac{\gamma-a}{\beta g h_2} - \frac{a}{(1-\beta)h_2}, \tag{23c}$$

$$x_{1b} = \frac{\xi}{e} - \frac{a}{(1-\beta)h_2}. \tag{23d}$$

Proof: We present the optimal solution to inner problem P3 based on the Lagrange method when a and β are given. The Lagrangian function for problem P3 is written as

$$L_1(x, y, z, \lambda_1, \lambda_2, \lambda_3, \lambda_4, \lambda_5) = x + y + z + \lambda_1(a h_1 y + a - h_1 x)$$

$$+ \lambda_2\left(\frac{\gamma-a}{\beta g} - h_2(x+y+z)\right) + \lambda_3\left(\frac{\gamma}{(1-\beta)} - h_2 x + \gamma h_2 y\right)$$

$$+ \lambda_4\left(\frac{a}{(1-\beta)} - h_2 y\right) + \lambda_5(\xi - e(x+y+z)), \tag{24}$$

where $\lambda_1 \geq 0, \lambda_2 \geq 0, \lambda_3 \geq 0, \lambda_4 \geq 0,$ and $\lambda_5 \geq 0$ are the Lagrangian multipliers associated with the corresponding constraints (18b), (18c), (18d), (18e) and (18f), respectively. Based on Lagrange function (24), the KKT optimality conditions can be written as follows:

$$\frac{dL_1}{dx} = 1 - \lambda_1 h_1 - \lambda_2 h_2 - \lambda_3 h_2 - \lambda_5 e = 0, \tag{25a}$$

$$\frac{dL_1}{dy} = 1 + \lambda_1 a h_1 - \lambda_2 h_2 + \lambda_3 \gamma h_2 - \lambda_4 h_2 - \lambda_5 e = 0, \tag{25b}$$

$$\frac{dL_1}{dz} = 1 - \lambda_2 h_2 - \lambda_5 e = 0, \tag{25c}$$

$$\lambda_1 (a h_1 y + a - h_1 x) = 0, \tag{25d}$$

$$\lambda_2 \left(\frac{\gamma - a}{\beta g} - h_2(x + y + z) \right) = 0, \tag{25e}$$

$$\lambda_3 \left(\frac{\gamma}{(1 - \beta)} - h_2 x + \gamma h_2 y \right) = 0, \tag{25f}$$

$$\lambda_4 \left(\frac{a}{1 - \beta} - h_2 y \right) = 0, \tag{25g}$$

$$\lambda_5 (\xi - e(x + y + z)) = 0, \tag{25h}$$

$$\lambda_1, \lambda_2, \lambda_3, \lambda_4, \lambda_5 \geq 0, \tag{25i}$$

$$(18b), (18c), (18d), (18e), (18f), (18g).$$

In order to get the solution of the five Lagrangian multipliers variables $\lambda_1, \lambda_2, \lambda_3, \lambda_4, \lambda_5$, we consider the system of equations composed by (25a), (25b) and (25c). To solve the system of equations, we select the variables λ_4 and λ_5 and we consider two general values of λ_4 and λ_5, i.e. $\lambda_4 = 0, \lambda_4 \neq 0, \lambda_5 = 0, \lambda_5 \neq 0$. In the following, we analyse the possible combinations for the solutions of the Lagrange multipliers by consider four cases based on λ_4 and λ_5.

Case 1: At first, let us consider the case that Lagrange multiplier $\lambda_4 = 0,$ and $\lambda_5 = 0,$ and then find the optimal solution to transmit power x, y and z.

If we set $\lambda_5 = 0$ in (25c), and $\lambda_4 = 0$ in (25b), we can solve the equation system composed by (25a), (25b), and (25c) to obtain solution $\lambda_1 = 0, \lambda_2 = 1/h_2,$ and $\lambda_3 = 0$. In this way, it is easy to see that the results of all Lagrangian multipliers meet the KKT optimality conditions shown in (25a), (25b) and (25c). Since $\lambda_1, \lambda_3, \lambda_4, \lambda_5 = 0$, we also meet conditions (25d), (25f), (25g), (25h) and (25i). Then, since λ_2 is greater than zero, from (25e), we establish that

$$\frac{\gamma - a}{\beta g} - h_2(x + y + z) = 0. \tag{26}$$

From (26), we derive $x + y + z$ and replace it in condition (18f); then, we reach the following inequality (27):

$$\xi - e\left(\frac{\gamma - a}{\beta g h_2}\right) \leq 0. \tag{27}$$

According to by (26) and (27), we notice that KKT conditions (18c) and (18f) are satisfied, respectively. When condition (27) is satisfied, we want to guarantee that the value of z will not be less than zero. From (26), if we derive variable z and make this expression greater than zero, we obtain the following expression:

$$x + y \leq \frac{\gamma - a}{\beta g h_2}. \tag{28}$$

Now, we proceed to derive variable y from the constraints of problem P3: (18b), (18d), (18e) and from condition (28), in order to obtain conditions (29a), (29b), (29c) and (29d).

$$y \leq \frac{x}{a} - \frac{1}{h_1}, \tag{29a}$$

$$y \leq \frac{x}{\gamma} - \frac{1}{(1 - \beta)h_2}, \tag{29b}$$

$$y \geq \frac{a}{(1 - \beta)h_2}, \tag{29c}$$

$$y \leq \frac{\gamma - a}{\beta g h_2} - x. \tag{29d}$$

Denote $y_1(x) = \frac{x}{a} - \frac{1}{h_1}$, $y_2(x) = \frac{x}{\gamma} - \frac{1}{(1-\beta)h_2}$, $y_3(x) = \frac{a}{(1-\beta)h_2}$, $y_{4a} = \frac{\gamma - a}{\beta g h_2} - x$, as the boundaries of (29a), (29b), (29c) and (29d), respectively.

We can see from Figure 3 that the intersection point of $y_2(x)$ and $y_3(x)$ results in point x_1, which is defined in equation (23a). And we can see from Figure 4 that x_2 is defined by the intersection point of $y_1(x)$ and $y_3(x)$, which is defined in (23b). Therefore, we consider two options: when $x_1 > x_2$, and when $x_2 \geq x_1$, as indicated in Figure 3 and Figure 4, respectively.

Accordingly, the intersection point of $y_{4a}(x)$ with $y_3(x)$ can be defined by x_{1a}, as expressed in (23 c). Then, when $x_1 > x_2$, we determine that problem P3 is feasible if $x_1 \leq x_{1a}$, and when $x_1 > x_2$, we determine that problem P3 is feasible if $x_2 \leq x_{1a}$. Since all the KKT conditions are satisfied, we can state that x_1 or x_2 represent one of the optimal transmit power control values, x^*, when $x_1 > x_2$ or $x_2 \geq x_1$, respectively. In the same way, we establish that $y_3(x)$ indicated in equation (21b), represents an optimal value for y^* that minimises the objective function of problem P3. For optimal transmit power control variable z^*, we derive z from equation (26), and we procced to replace the optimal x^* (i.e. x_1 or x_2) and y^* (i.e. $y_3(x)$ represented in (21b)) obtained in the previous steps as follows:
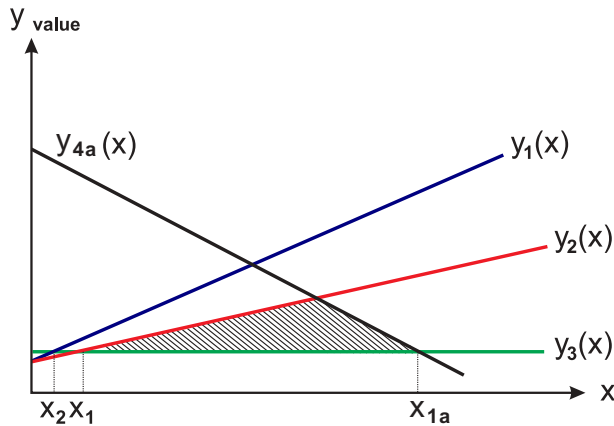
Figure 3. Diagram of the feasible region of problem P3 with $x_1 > x_2$.
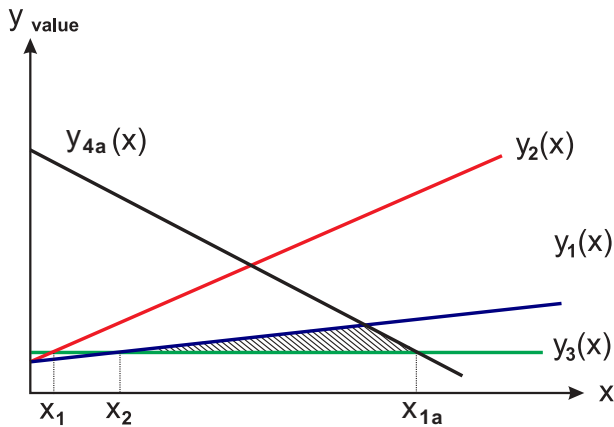

Figure 4. Diagram of the feasible region of problem P3 with $x_2 > x_1$.

$$z^* = \begin{cases} \frac{y-a}{\beta g h_2} - x_1 - y^*, & \text{if } x_1 > x_2, \quad\quad (30a) \\ \frac{y-a}{\beta g h_2} - x_2 - y^*, & \text{otherwise.} \quad\quad (30b) \end{cases}$$

Case 2: Secondly, let us consider the case that Lagrange multiplier $\lambda_4 = 0$, and $\lambda_5 \neq 0$, and then find the optimal solution to transmit power x, y and z.

If we set $\lambda_2 = 0$ in (25c), and $\lambda_4 = 0$ in (25b), we can solve the equation system composed by (25a), (25b) and (25c) to obtain the solution $\lambda_5 = 1/2$, $\lambda_1 = 0$ and $\lambda_3 = 0$. In this way, it is easy to see that the results of all Lagrangian multipliers meet the KKT optimality conditions shown in (25a), (25b) and (25c). Since $\lambda_1, \lambda_2, \lambda_3, \lambda_4, \lambda_5 = 0$, we also meet conditions (25d), (25e), (25f), (25g) and (25i).

Since λ_5 is greater than zero, from (25h), we establish that:

$$\xi - e(x + y + z) = 0. \quad\quad (31)$$

If we replace the result from deriving the term $x + y + z$ from (31) in constraint (18c), we have the following:

$$\frac{\gamma - a}{\beta g h_2} < \frac{\xi}{e}. \tag{32}$$

By arranging the terms in (32), we arrive at the following expression:

$$\xi - e\left(\frac{\gamma - a}{\beta g h_2}\right) \geq 0. \tag{33}$$

It is easy to see that condition (33) is the complement of condition (27). Therefore, the solution of this Case 2 is the complement of the solution obtained in the previous Case 1.

Now, we want to guarantee that the value of z does not become less than zero. Therefore, based on (31), the following inequality must be satisfied:

$$x + y \leq \frac{\xi}{e}. \tag{34}$$

Similar to the previous Case 1, we proceed to derive variable y from the constraints of problem P3: (18b), (18d) and (18e). In this case, we consider condition (34) to avoid negative values of power control variable z. Hence, we obtain conditions (29a), (29b), (29c) and (35):

$$y \leq \frac{\xi}{e} - x. \tag{35}$$

Denote $y_{4b}(x) = \frac{\xi}{e} - x$ as the boundary of (35).

We can see from Figure 5 and Figure 6 that the point where $y_{4b}(x)$ intersects with $y_3(x)$ can be defined by x_{1b}, as indicated in (23d).

Then, when $x_1 > x_2$, we determined that problem P3 is feasible if $x_1 \leq x_{1b}$, whereas when $x_2 \geq x_1$, we determined that problem P3 is feasible if $x_2 \leq x_{1b}$. In this sense, we can establish that x_1 or x_2 represent one of the optimal transmit power control values, x^*, when $x_1 > x_2$ or $x_2 \geq x_1$, respectively. Besides, $y_3(x)$ indicated in equation (21b), represents an optimal value for y^* that minimises the objective function of problem P3.
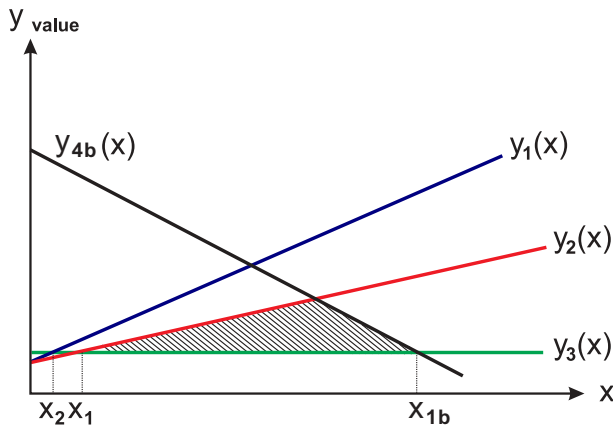

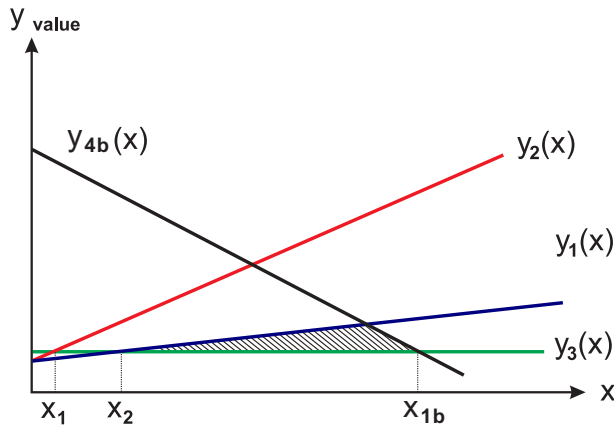Figure 5. Diagram of the feasible region of problem P3 with $x_1 > x_2$.

Figure 6. Diagram of the feasible region of problem P3 with $x_2 > x_1$.

As for power control variable z^*, we proceed to replace the optimal power control values of x^* (i.e. x_1 or x_2) and y^* (i.e. $y_3(x)$) in (31), which can be expressed as follows:

$$z^* = \begin{cases} \frac{\xi}{e} - x_1 - y^*, & \text{if } x_1 > x_2, \qquad (36a) \\ \frac{\xi}{e} - x_2 - y^*, & \text{otherwise.} \qquad (36b) \end{cases}$$

Subsequently, we can conclude that one of the optimal values of x^* will be the maximum between x_1 and x_2. As well, the optimal y^* will be $y_3(x)$ given x_1 or x_2 as the optimal x^*, as we show in (21a) and (21b). Furthermore, z^* can be defined by (21c), depending on whether condition (27) is satisfied or not.

Case 3: Thirdly, let us consider the case that Lagrange multiplier $\lambda_4 \neq 0$, and $\lambda_5 = 0$, and then find the optimal solution to transmit power x, y and z.

If $\lambda_5 = 0$, from (25c), we obtain $\lambda_2 = 1/h_2$. Then, if we replace the value of λ_2 in (25a), we obtain the following equation:

$$- \lambda_1 h_1 = \lambda_3 h_2. \qquad (37)$$

Since $\lambda_1, \lambda_3, h_1, h_2 \geq 0$, the unique possible solution is $\lambda_1 = \lambda_3 = 0$. Then, if we replace $\lambda_1 = \lambda_3 = 0$ in (25b), it results in $\lambda_4 = 0$, which contradicts the Lagrange multipliers, $\lambda_4 \neq 0$, and $\lambda_5 = 0$ considered in this Case 3. Hence, it is impossible to satisfy the set of Lagrange multipliers composed by $\lambda_4 \neq 0$, and $\lambda_5 = 0$.

Case 4: Lastly, let us consider the case that Lagrange multiplier $\lambda_4 \neq 0$, and $\lambda_5 \neq 0$, and then find the optimal solution to transmit power x, y and z.

If $\lambda_5 \neq 0$ from (25c), we have two possibilities. The first is when $\lambda_2 \neq 0$, and the second is when $\lambda_2 = 0$.

When $\lambda_2 \neq 0$, if we derive λ_5 from (25d), we obtain the following:

$$\lambda_5 = 1 - \lambda_2 h_2. \qquad (38)$$

Then, if we replace (38) in (25a), we obtain equation (37). Like the previous case, since $\lambda_1, \lambda_3, h_1, h_2 \geq 0$, the unique possible solution is $\lambda_1 = \lambda_3 = 0$. However, replacing (38) and

$\lambda_1 = \lambda_3 = 0$ in (25b) results in $\lambda_4 = 0$, which contradicts the Lagrange multiplier $\lambda_4 \neq 0$ proposed in this Case 4.

When $\lambda_2 = 0$, we obtain $\lambda_5 = 1/e$ from (25c). Then, replacing λ_2 and λ_5 in (25a), we obtain equation (37), the same as before, and since $\lambda_1, \lambda_3, h_1, h_2 \geq 0$, the unique possible solution is $\lambda_1 = \lambda_3 = 0$. But replacing $\lambda_1, \lambda_2, \lambda_3, \lambda_5$ in (25b) again results in $\lambda_4 = 0$, which contradicts the Lagrange multipliers, $\lambda_4 \neq 0, \lambda_5 \neq 0$ proposed in this Case 4. Hence, it is impossible to satisfy the set of Lagrange multipliers composed of $\lambda_4 \neq 0$, and $\lambda_5 \neq 0$. Thus, Proposition 1 is completely proved since all the KKT conditions were satisfied.

Note that we send a separate signal to the user that solely harvests energy because we would like to analyse the general case where the energy signal is separate to adjust the energy level or to satisfy the required minimum harvested energy level. Moreover, in the proposed solution there are various optimal solutions that satisfy the KKT conditions as we mention in the Section 3.1 through the proof of the Proposition 1. For instance, the case of $z = 0$ (when the energy signal is not used) is one of the possible optimal solutions considered in the proposed scheme. Specifically, we can see that the EH signal is zero along $y_{4a}(x)$ and $y_{4b}(x)$ since these lines represent the boundaries for the condition of $z \geq 0$ given in (28) and (34). Then, from the Figure 3, and Figure 4, we can see that the intersection of $y_{4a}(x)$ with $y_3(x)$ results in the point x_{1a} which corresponds to one solution when the EH signal is equal to zero for the Case 1 of the proof in the Proposition 1. As well as, from the Figure 5, and Figure 6, the intersection of $y_{4b}(x)$ with $y_3(x)$ results in the point x_{1b} which corresponds to another solution when the energy EH signal is equal to zero for the Case 2 of the proof in Proposition 1.

The inner optimisation problem is solved by applying Lagrange method to find the closed-form expressions for the power allocation variables x, y, and z for user 1, user 2 and user 3, respectively. Subsequently, a greater number of closed-form expressions that satisfy the KKT conditions are required for the new power allocation variables for each user when a larger number of users are involved in the network. However, it is possible to adapt our proposed solution in a grouping-based NOMA system (Lim & Ko, 2015) where the number of users was divided into groups composed of two users. Since each group is based on the distance between the transmitter and each user, we have a similar system model proposed in this paper. In this way, the proposed solution can be applied to each group at the cost of spectral efficiency where each group in the grouping-based NOMA system can use a portion of the total bandwidth or can be separated in time such that there is no interference between groups.

3.2. Solution for the outer minimisation problem

Afterwards, to complete the bi-level optimisation task, the optimal β and a can be found by using the exhaustive search method. However, this method takes a long time due to its very high computational complexity (Tuan & Koo, 2017a). Therefore, motivated by the advantages of PSO algorithm providing lower computational complexity than the exhaustive search method and fast convergence and high precision compared to other search methods such as ant colony optimisation, genetic algorithm, and so on, in the paper we utilise a PSO-based algorithm (Robinson & Rahmat-Samii, 2004; Zhang et al., 2015). PSO is an evolutionary and iterative algorithm based on swarm intelligence that has been successfully applied to solve optimisation problems of wireless communications. Some

examples are as following: In the reference (Tuan & Koo, 2017b), PSO was combined with semidefinite relaxation (SDR) technique to find the optimal beamforming vectors and power splitting ratios in a SWIPT cognitive radio networks. In addition, Garcia et al. (2019) proposed a PSO-based power allocation scheme for secrecy sum rate maximisation in NOMA with cooperative relaying system. A multi-user MISO SWIPT system with rate-splitting multiple access (RSMA) was proposed by Camana et al. (2019), where the minimum transmit power problem subject to QoS and EH constraints is solved with a PSO-based algorithm combined with the SDR- or successive convex approximation (SCA)-based approaches.

Let MI and NP denote as the maximum number of iterations and the number of particles in a swarm, respectively. Each particle's position is a vector composed of β and a values. The updating of each particle's position $f(\mathbf{x}_m)$ in each iteration is oriented towards the global and local best positions. Let us denote the global best position as $\mathbf{g}_b$, which conforms to g_{b1} and g_{b2} for β and a, respectively. Similarly, let us denote the local best position as $\mathbf{p}_{b,m}$, which conforms to $p_{b,m1}$, and $p_{b,m2}$, for β and a, respectively. We define the objective function $f(\mathbf{x}_m)$ as the value of 18(a), obtained by solving the inner optimisation problem P3 with the Proposition 1, when the set of β and a values are $\beta = \mathbf{x}_m(1)$ and $a = \mathbf{x}_m(2)$, respectively. The $\mathbf{g}_b$ values of the β and a variables are evaluated by updating the velocity $\mathbf{v}_m$ and position $\mathbf{x}_m$ of each particle until the minimum value of $f(\mathbf{x}_m)$ is obtained. The inertia weight for the velocity update is denoted by i_w, and the cognitive and social parameters are denoted by c_1 and c_2 as scaling factors, respectively.

The value of a_{max} is obtained based on the constraint (17b) as follows:

$$a_{\max} = h_1 x_{\max}, \tag{39a}$$

$$a_{\max} = h_1 P_{\max}, \tag{39b}$$

where $P_{\max}$ represents the maximum power available at the transmitter, which is used to limit the maximum value of the power control variable x.

The value of a_{min} is obtained based on the constraint (17c) considering $a \geq 0$ as follows:

$$a_{\min} \geq \gamma - gh_2(x + y + z), \tag{40a}$$

$$a_{\min} \geq \gamma - gh_2 P_{\max}, \tag{40b}$$

$$a_{\min} = \max(0, \gamma - gh_2 P_{\max}). \tag{40c}$$

Finally, the proposed algorithm based on PSO to solve outer minimisation problem of problem P3 can be summarised in Table 1.

4. Problem formulation and solution for OMA

In this section, for comparison purposes, we consider the power allocation problem for OMA with an energy-harvesting user. Vaezi et al. (2019) in the Subsection 5.3 established that the TDMA and frequency-division multiple access (FDMA) technique in OMA have the same performance in term of the capacity regions in a single cell network composed of one BS and two users. In particular, the TDMA technique dedicated a fraction A_1 of the

Table 1. The proposed algorithm based on PSO to solve problem P3.

1:	**inputs**: MI, NP, v_{max}, a_{min}, a_{max} c_1, c_2, and variables $\{\mathbf{x}_m\}$, $m = 1, ..., NP$.
2:	Initialisation
3:	Set the iteration index of the PSO loop: $r = 1$.
4:	Set initial values for elements of $\mathbf{x}_m(1)$ and $\mathbf{x}_m(2)$, , which are randomly selected in $(0, 1)$ and $[a_{min}, a_{max}]$, respectively, and calculate $f(\mathbf{x}_m)$ by solving the inner optimisation problem P3.
5:	Set the initial global best solution: $\mathbf{g}_b = \arg\min_{1 \leq NP} f(\mathbf{x}_m)$.
6:	Set the initial particle's best position: $\mathbf{p}_{b,m} = \mathbf{x}_m,$.
7:	Initialise the particle's velocity: $\mathbf{v}_m = 0,$.
8:	**while** $r \leq MI$ **do**
9:	**for** $m = 1 : NP$ **do**
10:	Calculate particle's new velocity: $$\mathbf{v}_m \leftarrow i_m \mathbf{v}_m + c_1 \pi_{1,m} (\mathbf{p}_{b,m} - \mathbf{x}_m) + c_2 \pi_{2,m} (\mathbf{g}_b - \mathbf{x}_m)$$ where $\pi_{1,m}, \pi_{2,m}$ are independently uniformly distributed vectors in $[0, 1]$.
11:	Limit each element of vector $\mathbf{v}_m$ in $[-v_{max}, v_{max}]$.
12:	Calculate the particle's position update: $\mathbf{x}_m \leftarrow \mathbf{x}_m + \mathbf{v}_m$.
13:	Set the threshold of each element of vector $\mathbf{x}_m(1)$ in $(0, 1)$ and $\mathbf{x}_m(2)$ in $[a_{min}, a_{max}]$.
14:	Calculate $f(\mathbf{x}_m)$ and the corresponding optimal values of x^*, y^*, z^* by solving inner optimisation problem P3 when the set of β and a values are $\beta = \mathbf{x}_m(1)$ and $a = \mathbf{x}_m(2)$, respectively.
15:	Update the new best particle's position: **if** $f(\mathbf{x}_m) < f(\mathbf{p}_{b,m})$ **then** Update: $\mathbf{p}_{b,m} \leftarrow \mathbf{x}_m$. **end if**
16:	Update the global best position of the particle: **if** $f(\mathbf{x}_m) < f(\mathbf{g}_b)$ **then** Update: $\mathbf{g}_b \leftarrow \mathbf{x}_m$, $\{x^*, y^*, z^*\} \leftarrow \{x, y, z\}_m$. **end if**
17:	**end for**
18:	Update: $r \leftarrow r + 1$.
19:	**end while**
20:	**outputs**: $f(\mathbf{g}_b)$ is the minimum value of problem P2 at the optimal values $\{\beta^*, a^*\} = \mathbf{g}_b$, and the optimal transmit power control variables $\{x^*, y^*, z^*\}$.

time ($0 \leq A_1 \leq 1$) to user 1 and a fraction $(1 - A_1)$ of the time to user 2, where the total available power at the transmitter can be allocated to user 1 and user 2 in their respective time fractions. On the other hand, in the FDMA, the total bandwidth resource and the total available power at the transmitter are shared among the users. In addition, the TDMA technique has been commonly adopted in the literature (Cui et al., 2016; Oviedo & Sadjadpour, 2016; Tabassum, Ali, Hossain, Hossain et al., 2017; Xu et al., 2017, September) for the purpose of performance comparisons with OMA. Therefore, in the paper we consider TDMA in OMA.

In this case, the system operates in TDMA mode, and the time resource is allocated to user 1 and user 2. The objective is to minimise the transmitted power under the constraint of minimum EH and minimum data rates required at user 1 and user 2. Subsequently, we can get the following optimisation problem P4 for OMA.

$$P4: \min_{\{A_1, p_1, p_2\}} p_1 + p_2 \tag{41a}$$

$$\text{s.t. } A_1 \log_2(1 + SNR_1) \geq c_1, \tag{41b}$$

$$(1 - A_1) \log_2(1 + SNR_2) \geq c_2, \tag{41c}$$

$$EH \geq \xi, \tag{41d}$$

$$0 < A_1 < 1, \tag{41e}$$

where A_1 indicates the fraction time assigned to user 1, $(1 - A_1)$ is the fraction time assigned to user 2, c_1 is the target data rate at user 1, c_2 is the target data rate at user 2, and p_1 and p_2 are the transmit power control variables for user 1 and user 2, respectively. The SNR corresponding to user 1 and user 2 are expressed in (42) and (43), respectively:

$$SNR_1 = \frac{|\tilde{h}_1|^2 p_1}{\sigma_1^2}, \tag{42}$$

$$SNR_2 = \frac{|\tilde{h}_2|^2 p_2}{\sigma_2^2}. \tag{43}$$

The energy harvested at user 3 can be given by

$$EH = |\tilde{e}|^2(A_1 p_1 + (1 - A_1)p_2) = e_2(A_1 p_1 + (1 - A_1)p_2), \tag{44}$$

where $e_2 = |\tilde{e}|^2$.

Optimisation problem P4 above is non-convex since the fraction time for user 1, A_1, is coupled with transmit powers p_1 and p_2 in constraints (41b), (41c) and (41d). Similar to the case of NOMA, to overcome this problem, we transform P4 into bi-level optimisation problem P5 (with upper-level variable A_1) as follows:

$$P5: \min_{A_1}\left(h(A_1) = \min_{p_1, p_2} p_1 + p_2\right) \tag{45a}$$

$$\text{s.t. } -\frac{h_1 p_1}{\sigma_1^2 \varphi_1} + 1 \leq 0, \tag{45b}$$

$$-\frac{h_2 p_2}{\sigma_2^2 \varphi_2} + 1 \leq 0, \tag{45c}$$

$$\xi - (A_1 e_2 p_1) - (1 - A_1)(e_2 p_2) \leq 0, \tag{45d}$$

$$p_1, p_2 \geq 0, \tag{45e}$$

where $h_1 = |\tilde{h}_1|^2$, $h_2 = |\tilde{h}_2|^2$, $\varphi_1 = 2^{\frac{c_1}{A_1}} - 1$, $\varphi_2 = 2^{\frac{c_2}{(1-A_1)}} - 1$, and $h(A_1)$ is the inner optimisation problem with respect to variables p_1 and p_2.

Similarly to the case of cooperative NOMA, to solve the problem P5, at first we will obtain the optimal solution for power control variables p_1 and p_2 based on the Lagrange method, since the inner problem P5 in (45) is convex. After that, we utilise a PSO-based method in order to find the optimal solution related to upper-level variable A_1. In the following subsection, we will provide more detailed description on solutions for the inner and outer minimisation problem.

Note that the β variable does not use in the formulated optimisation problem in OMA since this would involve an additional slot time dedicated to the cooperative phase. In particular, the total transmit power of the transmitter can be used to send the message s_1 to user 1 without interference of the message s_2 (in the case of NOMA during the phase A, the received SINR at user 1 has the interference of the message s_2 as we indicated in (2)). Then, the required rate at user 1 in OMA can be satisfied without the necessity of a cooperative phase.

The minimum SINR γ for user 1 and the minimum SNR a for user 2 do not use in the problem formulation of OMA. Instead, we define a minimum rate c_1 for user 1 and c_2 for user 2. In addition, in OMA we consider the fraction time assigned to each user as optimisation variable.

4.1. Solution for the inner minimisation problem with OMA

First, let us describe the solution for lower-level variables of the inner optimisation problem P5 by using Proposition 2.

Proposition 2: For inner problem P5, we define the optimal solution transmit power for p_1 and p_2, denoted as p_1^* and p_2^*, respectively. According to the below proof, p_1^* and p_2^* can be given as following, when A_1 is given.

Instance 1: if $p_{1b} \geq p_{1a}$,

$$p_1^* = \begin{cases} p_{1b}, & \text{if } 2A_1 \geq 1, & (46a) \\ p_{1a}, & \text{if } 2A_1 < 1. & (46b) \end{cases}$$

$$p_2^* = \begin{cases} p_{2b}, & \text{if } 2A_1 \geq 1, & (46c) \\ p_{2a}, & \text{if } 2A_1 < 1. & (46d) \end{cases}$$

Instance 2: if $p_{1b} < p_{1a}$,

$$p_1^* = p_{1a}, \tag{46e}$$

$$p_2^* = p_{2a}, \tag{46f}$$

where

$$p_{1a} = \frac{\sigma_1^2 \varphi_1}{h_1}, \tag{47a}$$

$$p_{1b} = \left[\xi - (1 - A_1) \left(\frac{e_2 \sigma_2^2 \varphi_2}{h_2} \right) \right] \frac{1}{e_2 A_1}, \tag{47b}$$

$$p_{2a} = \frac{\sigma_2^2 \varphi_2}{h_2}, \tag{47c}$$

$$p_{2b} = \left[\xi - A_1 \left(\frac{e_2 \sigma_1^2 \varphi_1}{h_1} \right) \right] \frac{1}{e_2 (1 - A_1)}. \tag{47d}$$

Proof: We will derive the solution for inner problem P5 based on the Lagrange method. From the inner problem P5, Lagrangian function can be written as

$$L_2(p_1, p_2, \lambda_1, \lambda_2, \lambda_3) = p_1 + p_2 + \lambda_1 \left(-\frac{h_1 p_1}{\sigma_1^2 \varphi_1} + 1 \right)$$

$$+ \lambda_2 \left(-\frac{h_2 p_2}{\sigma_2^2 \varphi_2} + 1 \right) + \lambda_3 (\xi - A_1 e_2 p_1 - (1 - A_1)(e_2 p_2)), \tag{48}$$

where $\lambda_1 \geq 0$, $\lambda_2 \geq 0$ and $\lambda_3 \geq 0$ are the Lagrangian multipliers associated with the corresponding constraints, (45b), (45c) and (45d), respectively. Based on Lagrange function (48), the KKT optimality conditions can be written as follows:

$$\frac{\partial L_2}{\partial p_1} = 1 - \frac{\lambda_1 h_1}{\sigma_1^2 \varphi_1} - \lambda_3 A_1 e_2 = 0, \tag{49a}$$

$$\frac{\partial L_2}{\partial p_2} = 1 - \frac{\lambda_2 h_2}{\sigma_2^2 \varphi_2} - \lambda_3 (1 - A_1) e_2 = 0, \tag{49b}$$

$$\lambda_1 \left(-\frac{h_1 p_1}{\sigma_1^2 \varphi_1} + 1 \right) = 0, \tag{49c}$$

$$\lambda_2 \left(-\frac{h_2 p_2}{\sigma_2^2 \varphi_2} + 1 \right) = 0, \tag{49d}$$

$$\lambda_3 (\xi - A_1 (e_2 p_1) - (1 - A_1)(e_2 p_2)) = 0, \tag{49e}$$

$$(43b), (43c), (43d), (43e).$$

In order to get the solution of the three Lagrangian multipliers variables λ_1, λ_2 and λ_3, we consider the system of equations composed by (49a) and (49b). To solve the system of equations, we consider the cases of $\lambda_1 = 0$, $\lambda_1 \neq 0$, $\lambda_2 = 0$, $\lambda_2 \neq 0$, $\lambda_3 = 0$ and $\lambda_3 \neq 0$. In the following, we analyse all possible combinations for the solutions of the Lagrange multipliers variables by consider eight cases based on λ_1, λ_2 and λ_3.

Case 1: At first, let us consider the case that Lagrange multiplier $\lambda_1 = 0$, $\lambda_2 \neq 0$ and $\lambda_3 \neq 0$, and then find the optimal solution to transmit power p_1 and p_2.

If we set $\lambda_1 = 0$ in (49a), we can solve the equation system composed by (49a) and (49b), and we get the results of Lagrange multipliers $\lambda_3 = \frac{1}{e_2 A_1}$, and $\lambda_2 = \frac{\sigma_2^2 \varphi_2}{h_2} \left(1 - \frac{(1 - A_1)}{A_1} \right)$.

We satisfy the KKT optimality conditions shown in (49a), (49b) and (49c). Furthermore, since λ_2 is greater than zero, we reach the following condition:

$$2A_1 > 1. \tag{50}$$

Since λ_2 and $\lambda_3 \neq 0$, the constraints (45c) and (45d) must be equal to zero, and then, we can derive the optimal power control variable p_2^* (represented by p_{2a} in (47c)) from (45c), and p_1^* (represented by p_{1b} in (47b)) from (45c) and (45d). In order to satisfy the KKT condition (45b), we define p_{1a} as the value of the variable p_1 obtained through the boundary of condition (45b), and we need to guarantee $p_{1b} \geq p_{1a}$. Therefore, all KKT conditions are satisfied and the Case 1 is the optimal solution when $p_{1b} \geq p_{1a}$ and $2A_1 > 1$.

Case 2: Secondly, let us consider the case that Lagrange multiplier $\lambda_1 \neq 0$, $\lambda_2 = 0$ and $\lambda_3 \neq 0$, and then find the optimal solution to transmit power p_1 and p_2.

If we set $\lambda_2 = 0$ in (49b), we can solve the equation system composed by (49a) and (49b), and we get the results of Lagrangian multipliers $\lambda_3 = \frac{1}{e_2(1-A_1)}$ and $\lambda_1 = \frac{\sigma_1^2 \varphi_1}{h_1}\left(1 - \frac{A_1}{(1-A_1)}\right)$. Then, since λ_1 is greater than zero, we reach condition (51), which is complementary to condition (50):

$$2A_1 < 1. \tag{103}$$

Since $\lambda_1 \neq 0$ and $\lambda_3 \neq 0$, the constraint (45b) and (45d) must be equal to zero. So, we can derive the optimal power control variable p_1^* (represented by p_{1a} in (47a)) from (45b), and p_2^* (represented by p_{2b} in (47d)) from (45b) and (45d). In order to satisfy the KKT condition (45c), we define p_{2a} as the value of the variable p_2 obtained through the boundary of condition (45c), and we need to guarantee $p_{2b} \geq p_{2a}$. Therefore, all KKT conditions are satisfied and the Case 2 has the optimal solution when $p_{2b} \geq p_{2a}$ and $2A_1 < 1$.

Now, we proceed to derive variable p_1 from constraint (45b), and p_2 from constraints (45c) and (45d).

$$p_1 \geq \frac{\sigma_1^2 \varphi_1}{h_1}, \tag{52a}$$

$$p_2 \geq \frac{\sigma_2^2 \varphi_2}{h_2}, \tag{52b}$$

$$p_2 \geq [\xi - A_1(e_2 p_1)]\frac{1}{e_2(1 - A_1)}. \tag{52c}$$

Denote $b_1 = \frac{\sigma_1^2 \varphi_1}{h_1}$, $b_2 = \frac{\sigma_2^2 \varphi_2}{h_2}$, $b_3(p_1) = [\xi - A_1(e_2 p_1)]\frac{1}{e_2(1-A_1)}$, as the boundaries of (52a), (52b) and (52c), respectively.

We can see from Figure 7 that the intersection point of b_3 and b_2 results in p_{1b} equal to (47b) and p_{2a} equal to (47c). The intersection point of b_3 and b_1 results in p_{1a} equal to (47a) and p_{2b} equal to (47d). Furthermore, Figure 7 shows that if $p_{2b} \geq p_{2a}$ then $p_{1b} \geq p_{1a}$ and vice versa. Therefore, we can get Instance 1 of Proposition 2 for both Case 1 and 2.

Case 3: Thirdly, let us consider the case that Lagrange multiplier $\lambda_1 \neq 0$, $\lambda_2 \neq 0$ and $\lambda_3 = 0$, and then find the optimal solution to transmit power p_1 and p_2.

If we set $\lambda_1 \neq 0$, $\lambda_2 \neq 0$, the constraint (45b) and (45c) must be equal to zero, then, we can derive the optimal power control variable p_1^* as p_{1a} and p_2^* as p_{2a}. We can see from Figure 7
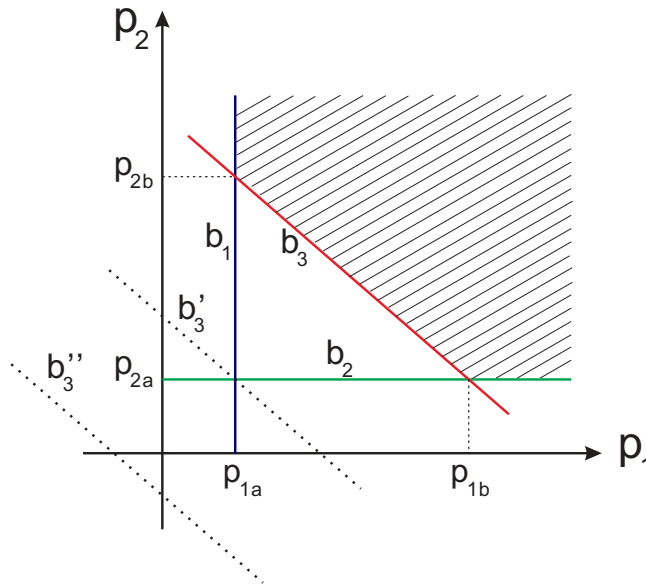
Figure 7. Diagram of the feasible region of problem P5.

that these solutions only are possible if boundary of the constraint (45d) is the position represented by b_3'', which also satisfy the KKT condition (45d). Therefore, in the Case 3, we will get the optimal solution if $p_{2b} < p_{2a}$, as given in the Instance 2 of Proposition 2.

Case 4: Fourthly, let us consider the case that Lagrange multiplier $\lambda_1 \neq 0$, $\lambda_2 \neq 0$, and $\lambda_3 \neq 0$, and then find the optimal solution to transmit power p_1 and p_2.

If we set $\lambda_1 \neq 0$, $\lambda_2 \neq 0$, and $\lambda_3 \neq 0$, the constraint (45b), (45c) and (45d) must be equal to zero. Hence, we get the optimal solution $p_1^* = p_{1a} = p_{1b}$, and $p_2^* = p_{2a} = p_{2b}$, when $p_{1a} = p_{1b}$ and $p_{2a} = p_{2b}$ to satisfy the constraint (45b), (45c) and (45d). This solution is possible when boundary b_3 goes through the intersection point of p_{1a} and p_{2a} (represented by b_3' in Figure 7).

Case 5: Fifthly, let us consider the case that Lagrange multiplier $\lambda_1 = 0$, $\lambda_2 = 0$ and $\lambda_3 \neq 0$, and then find the optimal solution to transmit power p_1 and p_2.

If we set $\lambda_1 = 0$, and $\lambda_2 = 0$, we get $\lambda_3 = \frac{1}{e_2 A_1}$ from (49a) and $\lambda_3 = \frac{1}{e_2(1-A_1)}$ from (49b). Hence, we need to satisfy the following condition.

$$2A_1 = 1. \tag{53}$$

We can see that Case 5 is the complement of Case 1 and Case 2 when $2A_1 = 1$. Therefore, the optimal solution of Case 5 is included in the Instance 1 of Proposition 2.

Case 6: Sixthly, let us consider the case that Lagrange multiplier $\lambda_1 = 0$, $\lambda_2 = 0$ and $\lambda_3 = 0$, and then find the optimal solution to transmit power p_1 and p_2.

From KKT condition (49a), if $\lambda_1 = 0$, then we cannot obtain $\lambda_3 = 0$, and vice versa. Therefore, the set of Lagrange multipliers proposed in this Case 6 is not a solution for the problem P5.

Case 7: Next, let us consider the case that Lagrange multiplier $\lambda_1 \neq 0$, $\lambda_2 = 0$ and $\lambda_3 = 0$, and then find the optimal solution to transmit power p_1 and p_2.

From KKT condition (49b), if $\lambda_2 = 0$, then we cannot obtain $\lambda_3 = 0$, and vice versa. Therefore, the set of Lagrange multipliers proposed in this Case 7 is not a solution for the problem P5.

Case 8: Lastly, let us consider the case that Lagrange multiplier $\lambda_1 = 0$, $\lambda_2 \neq 0$ and $\lambda_3 = 0$, and then find the optimal solution to transmit power p_1 and p_2.

From KKT condition (49a), if $\lambda_1 = 0$, then we cannot obtain $\lambda_3 = 0$, and vice versa. Therefore, the set of Lagrange multipliers proposed in this Case 8 is not a solution for the problem P5.

4.2. Solution for the outer minimisation problem with OMA

Afterwards, to complete the bi-level optimisation task, and to find the optimal A_1, we use the PSO-based algorithm. Similar to the case of NOMA in the Section 3, we denote *MI* as the maximum number of iterations and *NP* as the number of particles in a swarm. Each particle's position correspond to the value of A_1. The search range of A_1 is $(0, 1)$. The *m*th particle's position, velocity and local optimum position are denoted as x_m, v_m, and $p_{b,m}$, respectively. Denote as g_b the global best position for A_1 and $f(x_m)$ the minimum value obtained by solving the inner problem P5 by Proposition 2. The inertia weight for the velocity update is denoted by i_w, and the cognitive and social parameters represented are denoted by c_1 and c_2, respectively.

5. Numerical results

In this section, we present simulation results of the proposed scheme in terms of the transmit power. In addition, we provide the performance comparisons among the proposed scheme, conventional OMA and equal power splitting (EPS) (Tuan & Koo, 2017a). In the case of EPS scheme, β of 0.5 is used. So, the solution for the minimum transmit power of EPS is obtained by the problem P3 with $\beta = 0.5$.

We consider Rayleigh fading channels for $\widetilde{h}_1$, $\widetilde{h}_2$, $\tilde{g}$ and $\widetilde{e}$, and they have *i.i.d.* complex Gaussian distribution such that $\widetilde{h}_1 \sim \mathcal{CN}\left(0, d_{t,u_1}^{-\upsilon}\right)$, $\widetilde{h}_2 \sim \mathcal{CN}\left(0, d_{t,u_2}^{-\upsilon}\right)$, $\tilde{g} \sim \mathcal{CN}\left(0, d_{u_1 u_2}^{-\upsilon}\right)$ and $\widetilde{e} \sim \mathcal{CN}\left(0, d_{t,u_3}^{-\upsilon}\right)$, respectively, where d_{ij} denotes the distance between nodes i and j, and υ is the path-loss exponent; the index t_r indicates the transmitter, u_1 indicates user 1, u_2 indicates user 2, and u_3 indicates user 3. In the simulations, we use the value of the path-loss exponent $\upsilon = 4$ for channels $\widetilde{h}_1$, $\widetilde{h}_2$, $\tilde{g}$ and $\widetilde{e}$, and the noise power is given by $\sigma_1^2 = \sigma_2^2 = \sigma_3^2 = -60$ dBm. The distances between the nodes are the following: $d_{t,u_1} = 10$, $d_{t,u_2} = 5.5$, $d_{u_1 u_2} = 7.21$, and $d_{t,u_3} = 4$ in the unit of metre.

Figure 8 shows the convergence of the proposed PSO-based algorithm given in Table 1 in terms of the iteration index. As the iteration index is increased, the transmit power is improved. Moreover, Figure 8 shows that transmit power is convergent within about 40 iterations. Accordingly, we set the maximum number of iterations, *MI* to be 30 for the rest of our simulations. In addition to the value of *MI*, we set the swarm size $NP = 15$, scaling
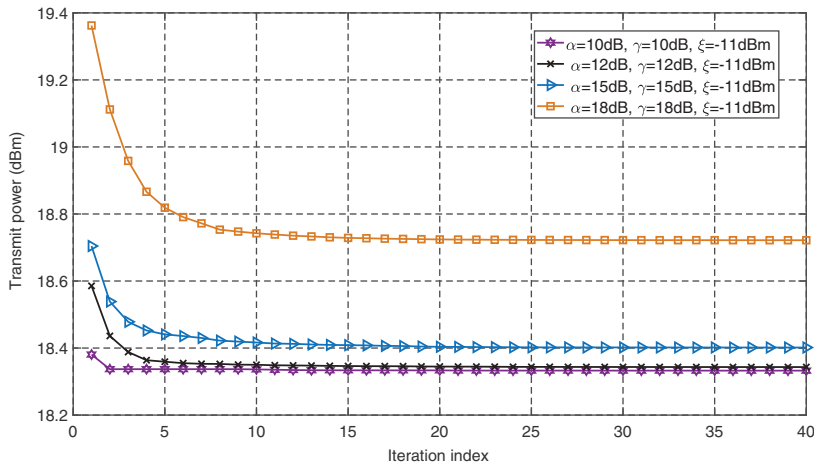
Figure 8. Convergence of the proposed algorithm with different required SINR, γ, SNR, α and minimum harvesting energy, ξ.
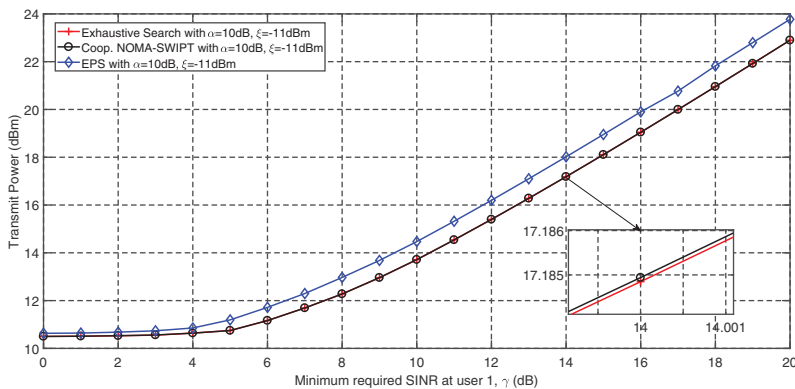

Figure 9. Transmit power comparison among exhaustive search, cooperative NOMA with SWIPT, and EPS at the transmitter according to the minimum required SINR, γ, at user 1.

factors $c_1 = 1.494$ and $c_2 = 1.494$, and inertia weight for the velocity update, $i_w = 0.7$ (Tuan & Koo, 2017a).

To check the optimality of the proposed algorithm, we investigated the results for problem P3 with a fixed SNR at user 2, $a = 10$ dB, a transmission time fraction $\tau = 0.5$ (Y. Xu et al., 2017, September), and the minimum power required by the energy-harvesting user, $\xi = -11$ dBm. Figure 9 shows the transmit power at the transmitter according to the minimum required SINR. From Figure 9, we can verify that the result obtained by the proposed algorithm can reach near-optimal performance, compared with the exhaustive search scheme. Different to the exhaustive search scheme, the proposed scheme aided with PSO-based method can reduce the time to reach for the optimal solution while, providing high accuracy with low computational complexity. For this simulation, we only utilised 10 channel realisations since the exhaustive search method requires a long time due to very high computational complexity. For this simulation, we only utilised 10
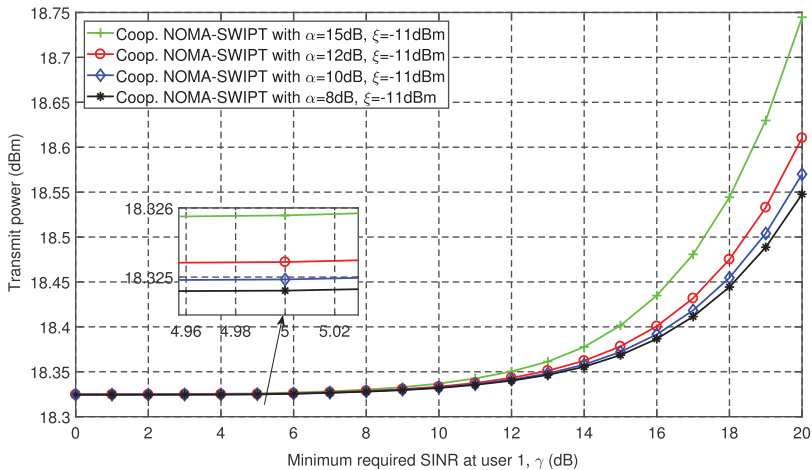
Figure 10. Transmit power at the transmitter according to the minimum SINR for user 1, γ.

channel realisations since the exhaustive search method requires a long time due to very high computational complexity. For the rest of simulation results, however 1000 channel realisations are used.

Figure 10 shows transmit power according to the minimum required SINR, γ, at user 1, which is obtained by the proposed scheme, when the minimum EH is $\xi = 11$ dBm and the minimum required SNR, α, is given as 15, 12, 10 and 8 dB at user 2, respectively. We can see that the transmit power increases with increasing values of the SINR because the transmitter should spend more power to data transfer so as to satisfy the required SINR by user 1. Moreover, there are slight changes of transmit power in the range of the low SINR requirement (i.e. less than 8 dB) because transmit power at the transmitter provides enough contribution to the SINR value under the EH constraint.

Figure 11 shows transmit power at the transmitter according to the minimum required SNR, α, at user 2 by the proposed scheme when the minimum EH $\xi = -11$ dBm and the minimum required SINR, γ, is given as 15, 12, 10 and 8 dB at user 1, respectively. Similar to
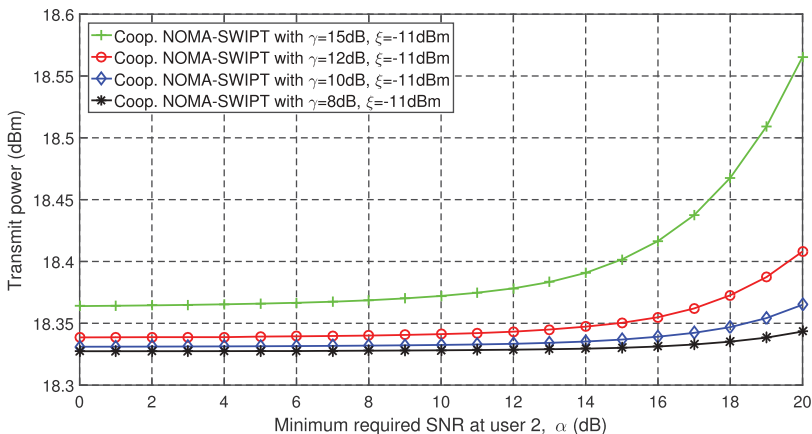

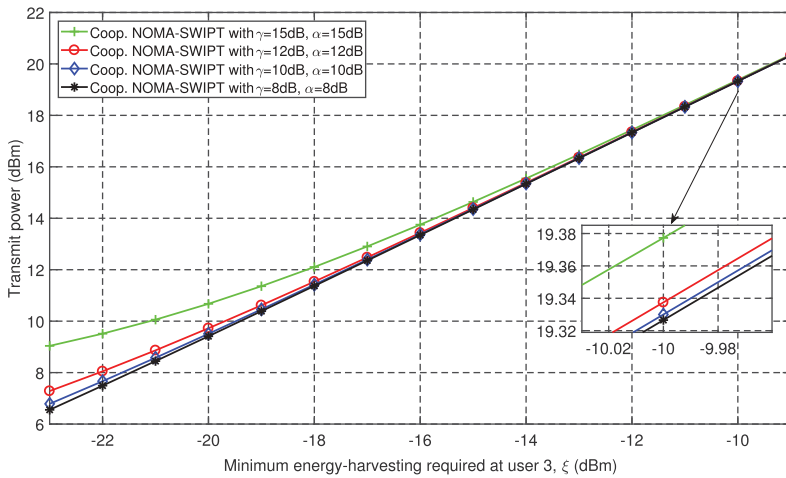**Figure 11.** Transmit power at the transmitter according to minimum SNR for user 2, α.

Figure 12. Transmit power at the transmitter according to minimum required EH, ξ.

Figure 10, the transmit power increases with increasing values for SNR because the transmitter has to deliver more power to satisfy the SNR needed by user 2.

Figure 12 shows the effect of the minimum harvested power on the transmit power at the transmitter when the required SINR at user 1 and SNR at user 2 are given. We observe that the transmit power increases with the more required EH because the transmitter should assign more power to the energy-harvesting user to satisfy the EH constraint. Furthermore, when the required SINRs at user 1 and user 2 increase, the total transmit power increases, as like observations in Figures 10 and 11. Therefore, the higher values for SINR and SNR requirements result in the more transmit power.

Figure 13 shows transmit power according to the target data rate of user 1, c_1, under OMA, cooperative NOMA with SWIPT and the EPS scheme for given fixed two different values of data rate of user 2 ($c_2 = 4$ bits/s/Hz and 6 bits/s/Hz), $\tau = 0.8$, and the minimum harvested power requirement $\xi = -18$. The performance gap among the three different
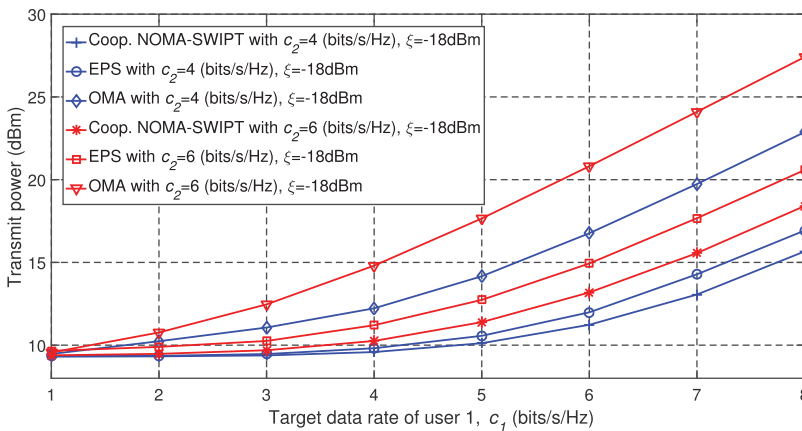

Figure 13. Transmit power comparison among cooperative NOMA with SWIPT, OMA and EPS according to the target data rate at user 1, c_1.

transmission schemes increases with the increasing target data rate of user 1. Subsequently, we know that cooperative NOMA with SWIPT provides lower transmit power than OMA and the EPS schemes.

6. Conclusion

In the paper, we studied an optimisation problem to find the minimum transmission power of a transmitter for a cooperative NOMA system with SWIPT while considering an energy-harvesting user. The transmit power is minimised subject to the constraints of minimum SINR at user 1, SNR at user 2, and minimum EH at user 3. Since the initial problem, P1, is not convex, we transformed it into a bilevel optimisation problem, P3. First, we solved the lower-level variables of the inner convex problem by using the Lagrange method and KKT optimality conditions. After that, we used PSO to find the values of the upper-level variables. Furthermore, we also studied the transmit power allocation for two baseline schemes: OMA and EPS for performance comparison. According to simulation results, it is shown that cooperative NOMA with SWIPT can reduce the transmit power at the transmitter, compared to two baseline schemes: OMA and EPS. As one of future works, energy efficiency maximisation will be very interesting topic where the objective function is the maximisation of the ratio of the achievable throughput to total energy consumption subject to some constraints. The study of NOMA-SWIPT scheme incorporated with single-input multiple-output (SIMO), multiple-input single-output (MISO) and multiple-input multiple-output (MIMO) antenna structures is also very interesting future work.

Disclosure statement

No potential conflict of interest was reported by the authors.

Funding

ORCID

Carla E. Garcia 🔾 http://orcid.org/0000-0003-4692-253X

References

Alsaba, Y., Leow, C. Y., & Abdul Rahim, S. K. (2018). Full-Duplex cooperative non-orthogonal multiple access with beamforming and energy harvesting. *IEEE Access*, *6*, 19726–19738. https://doi.org/10.1109/ACCESS.2018.2823723

Bi, S., Zeng, Y., & Zhang, R. (2016, April). Wireless powered communication networks: An overview. *IEEE Wireless Communications*, *23*(2), 10–18. https://doi.org/10.1109/MWC.2016.7462480

Camana, M. R., Tuan, P. V., Garcia, C. E., & Koo, I. (2019, August). Joint power allocation and power splitting for MISO SWIPT RSMA systems with energy-constrained users, 26(3), 2241–2254. *Wireless Networks*.

Camana, M. R., Tuan, P. V., & Koo, I. (2018, November). Optimised power allocation for a power beacon-assisted SWIPT system with a power-splitting receiver. *International Journal of Electronics*, *106*(3), 415–439. https://doi.org/10.1080/00207217.2018.1540063

Chen, Z., Ding, Z., Dai, X., & Zhang, R. (2017, October). An optimization perspective of the superiority of NOMA compared to conventional OMA. *IEEE Transactions on Signal Processing*, *65*(19), 5191–5202. https://doi.org/10.1109/TSP.2017.2725223

Clerckx, B., Zhang, R., Schober, R., Ng, D., Kim, D., & Poor, H. (2019, January). Fundamentals of wireless information and power transfer: From RF energy harvester models to signal and system designs. *IEEE Journal on Selected Areas in Communications*, *37*(1), 4–33. https://doi.org/10.1109/JSAC.2018.2872615

Cui, J., Ding, Z., & Fan, P. (2016). A novel power allocation scheme under outage constraints in NOMA systems. *IEEE Signal Processing Letters*, *23*(9), 1226–1230. https://doi.org/10.1109/LSP.2016.2591561

Diamantoulakis, P., Pappi, K., Ding, Z., & Karagiannidis, G. (2016, December). Wireless-powered communications with non-orthogonal multiple access. *IEEE Transactions on Wireless Communications*, *15*(12), 8422–8436. https://doi.org/10.1109/TWC.2016.2614937

Diamantoulakis, P., Pappi, K., & Karagiannidis, G. (2017, January). Joint downlink/uplink design for wireless powered networks with interference. *IEEE Access*, *5*, 1534–1547. https://doi.org/10.1109/ACCESS.2017.2657801

Ding, Z., Lei, X., Karagiannidis, G. K., Schober, R., Yuan, J., & Bhargava, V. K. (2017, October). A survey on non-orthogonal multiple access for 5G networks: Research challenges and future trends. *IEEE Journal on Selected Areas in Communications*, *35*(10), 2181–2195. https://doi.org/10.1109/JSAC.2017.2725519

Ding, Z., Peng, M., & Poor, H. V. (2015, August). Cooperative non-orthogonal multiple access in 5G systems. *IEEE Communications Letters*, *19*(8), 1462–1465. https://doi.org/10.1109/LCOMM.2015.2441064

Do, N., Da Costa, D., Duong, T., & An, B. (2017, March). A BNBF user selection scheme for NOMA-based cooperative relaying systems with SWIPT. *IEEE Communications Letters*, *21*(3), 664–667. https://doi.org/10.1109/LCOMM.2016.2631606

Garcia, C. E., Camana, M. R., Koo, I., & Rahman, M. A. (2019). Particle swarm optimization-based power allocation scheme for secrecy sum rate maximization in NOMA with cooperative relaying. *Lecture Notes in Computer Science*, 1–12. doi:10.1007/978-3-030-26969-2_1

Hanif, M. F., Ding, Z., Ratnarajah, T., & Karagiannidis, G. K. (2016, January). A minorization-maximization method for optimizing sum rate in the downlink of non-orthogonal multiple access systems. *IEEE Transactions on Signal Processing*, *64*(1), 76–88. https://doi.org/10.1109/TSP.2015.2480042

Islam, S. M. R., Avazov, N., Dobre, O. A., & Kwak, K. (2017). Power-domain Non-Orthogonal Multiple Access (NOMA) in 5G systems: Potentials and challenges. *IEEE Communications Surveys & Tutorials*, *19*(2), 721–742. https://doi.org/10.1109/COMST.2016.2621116

Krikidis, I., Timotheou, S., Nikolaou, S., Zheng, G., Ng, D., & Schober, R. (2014, November). Simultaneous wireless information and power transfer in modern communication systems. *IEEE Communications Magazine*, *52*(11), 104–110. https://doi.org/10.1109/MCOM.2014.6957150

Lim, S., & Ko, K. (2015). Non-Orthogonal Multiple Access (NOMA) to enhance capacity in 5G. *International Journal of Contents*, *11*(4), 38–43. https://doi.org/10.5392/IJoC.2015.11.4.038

Liu, Y., Ding, Z., Elkashlan, M., & Poor, H. V. (2016, April). Cooperative non-orthogonal multiple access with simultaneous wireless information and power transfer. *IEEE Journal on Selected Areas in Communications*, *34*(4), 938–953. https://doi.org/10.1109/JSAC.2016.2549378

Liu, Y., Qin, Z., Elkashlan, M., Ding, Z., Nallanathan, A., & Hanzo, L. (2017, December). Nonorthogonal multiple access for 5G and beyond. *Proceedings of the IEEE*, *105*(12), 2347–2381. https://doi.org/10.1109/JPROC.2017.2768666

Lv, L., Chen, J., Ni, Q., Ding, Z., & Jiang, H. (2018, April). Cognitive non-orthogonal multiple access with cooperative relaying: A new wireless frontier for 5G Spectrum sharing. *IEEE Communications Magazine*, *56*(4), 188–195. https://doi.org/10.1109/MCOM.2018.1700687

Mollanoori, M., & Ghaderi, M. (2011). On the complexity of wireless uplink scheduling with successive interference cancellation. *2011 49th Annual Allerton Conference on Communication, Control, and Computing (Allerton),* Monticello, IL, USA.

Nechibvute, A., Chawanda, A., Taruvinga, N., & Luhanga, P. (2017). Radio frequency energy harvesting sources. *Acta Electrotechnica et Informatica*, *17*(4), 19–27. https://doi.org/10.15546/aeei-2017-0030

Oviedo, J. A., & Sadjadpour, H. R. (2016). A new NOMA approach for fair power allocation. *2016 IEEE Conference on Computer Communications Workshops (INFOCOM WKSHPS),* San Francisco, CA, USA.

Ponnimbaduge Perera, T. D., Jayakody, D. N. K., Sharma, S. K., Chatzinotas, S., & Li, J. (2018). Simultaneous Wireless Information and Power Transfer (SWIPT): Recent advances and future challenges. *IEEE Communications Surveys and Tutorials*, *20*(1), 264–302. https://doi.org/10.1109/COMST.2017.2783901

Robinson, J., & Rahmat-Samii, Y. (2004, February). Particle swarm optimization in electromagnetics. *IEEE Transactions on Antennas and Propagation*, *52*(2), 397–407. https://doi.org/10.1109/TAP.2004.823969

Shi, Q., Peng, C., Xu, W., Hong, M., & Cai, Y. (2016, February). Energy efficiency optimization for MISO SWIPT systems with zero-forcing beamforming. *IEEE Transactions on Signal Processing*, *64*(4), 842–854. https://doi.org/10.1109/TSP.2015.2489603

Tabassum, H., Ali, M. S., Hossain, E., & Hossain, M. J. (2017). Modeling and analysis of uplink Non-Orthogonal Multiple Access (NOMA) in large-scale cellular networks using poisson cluster processes. *IEEE Transactions on Communications*, 1. https://doi.org/10.1109/TCOMM.2017.2699180

Tabassum, H., Ali, M. S., Hossain, E., Hossain, M. J., & Kim, D. I. (2017). Uplink vs. downlink NOMA in cellular networks: Challenges and research directions. *2017 IEEE 85th Vehicular Technology Conference (VTC Spring),* Sydney, NSW, Australia.

Tuan, P., & Koo, I. (2017a). Robust weighted sum harvested energy maximization for SWIPT Cognitive radio networks based on particle swarm optimization. *Sensors*, *17*(10), 2275. https://doi.org/10.3390/s17102275

Tuan, P. V., & Koo, I. (2017b). Optimal multiuser MISO beamforming for power-splitting SWIPT Cognitive radio networks. *IEEE Access*, *5*, 14141–14153. https://doi.org/10.1109/ACCESS.2017.2727073

Vaezi, M., Ding, Z., & Poor, H. V. (Eds.). (2019). *Multiple access techniques for 5G wireless networks and beyond*. Springer International Publishing. doi:10.1007/978-3-319-92090-0.

Xu, J., Liu, L., & Zhang, R. (2014, September). Multiuser MISO beamforming for simultaneous wireless information and power transfer. *IEEE Transactions on Signal Processing*, *62*(18), 4798–4810. https://doi.org/10.1109/TSP.2014.2340817

Xu, Y., Shen, C., Ding, Z., Sun, X., Yan, S., Zhu, G., & Zhong, Z. (2017, September). Joint beamforming and power-splitting control in downlink cooperative SWIPT NOMA systems. *IEEE Transactions on Signal Processing*, *65*(18), 4874–4886. https://doi.org/10.1109/TSP.2017.2715008

Yang, Z., Ding, Z., Fan, P., & Al-Dhahir, N. (2017, July). The impact of power allocation on cooperative non-orthogonal multiple access networks with SWIPT. *IEEE Transactions on Wireless Communications*, *16*(7), 4332–4343. https://doi.org/10.1109/TWC.2017.2697380

Zhai, D., Zhang, R., Cai, L., Li, B., & Jiang, Y. (2018, June). Energy-efficient user scheduling and power allocation for NOMA-based wireless networks with massive IoT devices. *IEEE Internet of Things Journal*, *5*(3), 1857–1868. https://doi.org/10.1109/JIOT.2018.2816597

Zhang, Y., Wang, S., & Ji, G. (2015). A comprehensive survey on particle swarm optimization algorithm and its applications. *Mathematical Problems in Engineering*, *2015*, 1–38. doi:10.1155/2015/931256

Zhou, F., Chu, Z., Sun, H., Hu, R. Q., & Hanzo, L. (2018, April). Artificial noise aided secure cognitive beamforming for cooperative MISO-NOMA using SWIPT. *IEEE Journal on Selected Areas in Communications*, *36*(4), 918–931. https://doi.org/10.1109/JSAC.2018.2824622